Збірник наукових праць. Галузеве машинобудування, будівництво
Academic journal. Industrial Machine Building, Civil Engineering
http://journals.nupp.edu.ua/znp
https://doi.org/10.26906/znp.2025.65.4212

UDC 624.012.35

Oleksandr Hryshchenko
National University of Water and Environment Engineering
https://orcid.org/0009-0004-1851-6571

Dmitro Kochkarev*
National University of Water and Environment Engineering
https://orcid.org/0000-0002-4525-7315

Invariance of reinforcement and concrete cohesion within the energy approach

Abstract. The work studies the problem of analytical description of reinforcement and concrete cohesion, which determines the malleability of loop joints and butt joints of prefabricated reinforced concrete structures. It also proves that existing empirical and semi-empirical models like 'tangential stresses – displacement' do not ensure accurate impact of common stress in reinforcement and are unable to describe the plastic stage of tenacity characterised by a transition to a quasi-uniform distribution of tangent stress along the anchoring length. The study suggests a universal analytical bond model built on a two-line chart 'τ–s' with a linear initial section where tangential stress depends on common stress in the reinforcement and a horizontal section that corresponds to the plastic stage. The level and the length of the plastic stage are determined due to the conditions for preserving the energy invariant of the bond. The writers suggest the energy criterion for the beginning of the saturation stage, understood as the equivalence state of intensity of elasto-plastic components' energy invariants. The resulting model allows the formation of physically justified bonding diagrams suitable for use in numerical methods for calculating the compliance of joints and butt joints.

Keywords: shear diagrams, models of reinforcement-concrete bond, shear deformations, bond parameters, average tangential bond stresses.
*Corresponding author E-mail: dim7@ukr.net

Received: 04.11.2025 Accepted: 05.12.2025 Published: 26.12.2025

Introduction.

The issue of considering the cohesion of reinforcement to concrete is pertinentfor calculating the hook joints of the prefabricated reinforced concrete structures, overall joint compliance of which is largely determined by the deformation properties of the reinforcement anchorage zone. In such joints, the transfer of forces between adjacent elements occurs primarily due to the performance of the reinforcement'scohesion with the concrete, rather thanthrough direct contact between the concrete surfaces. It causes increased sensitivity of the calculation results to the law of 'reinforcement-concrete' interaction.

In this regard, studying the mechanism of reinforcement cohesion in concrete and developing of adequate models of its deformation is one of the key tasks in determining the compliance of loop joints and butt joints of prefabricated reinforced concrete structures in general.Most scientific works aimed at the cohesion problem are focused on the experimental study of pulling outthe reinforcement bars [1, 3-5, 7] and the development of empirical and semi-empirical charts like 'tangential stresses – displacement' [11-16]. At the same time, most of the suggested dependencies are simplified and contain a significant number of empirical criteria, which, as a rule, do not consider the direct impact of the level of normal stressesin the reinforcement on the cohesion parameters and ignore energy approaches.

Some studies demonstrate that average tangential stresses of cohesion can be connected with normal stresses in the reinforcement through linear or quasi-linear dependenceuntill the slip zone along the anchorage length spreads [2, 6]. However, the subsequent stage of the cohesion operation, which is characterised by a change in the shape of the tangential stress diagram and a transition to a distribution close to rectangular, is practically not described in the present analytical models.

In this regard, there is a need to develop an analytical model of the cohesion of reinforcement to concrete based on energy approach that describes the complete process of the cohesion operation during pull,

including the plastic stage, and provides the development of physically based diagrams like «τ–s», suitable for use in numerical methods for calculating the compliance of joints.

It should be mentioned that the present normative shear diagrams [8–10], the parameters of which are obtained experimentally and empirically, have a limited scope of application and do not allow a reliable assessment of the parameters of the stress-strain state of reinforcement and concrete in the anchoring zone at a variable level of normal stresses.

Problem statement.

The research aims to develop a universal analytical model of cohesion of reinforcement to concrete that is based not on empirical selections of the curves, but on the fundamental principles of the energy balance.

Main material and results.

The limit point of the cohesion of reinforcement to concrete is determined not by the local values of tangential stresses and the form of their distribution along the anchorage length, but by the total specific energy transferred through the contact of reinforcement with concrete. This energy is an invariant quantity for a given pair of materials and exact cohesion conditions.

Overall, cohesion is a process of the contact area destruction that includes micro-shear of the concrete between ribs, opening of micro-cracks, local crushing of concrete, friction, and sliding. All those processes are energy-consuming. The maximum limit stress of cohesion τ_{max} can be reached locally, or not reached for short bars, or exceeded in some particular zones. In this case, contact destruction occurs only when sufficient work is done by the adhesion forces. That is why the criterion for the destruction of adhesion must be energetic.

$$G_{tot} = \int \tau(s) ds = const. \qquad (1)$$

It is the energy that should be considered as an invariant, as it does not depend on the anchoring length and the stress diagram form. For instance, the energy for long bars accumulates at the expense of stresses along the length, and for short bars, it is stored due to the deformation intensity, while invariant G remains stable. The stress diagrams may be of different forms, such as exponential, linear, and horizontal plots. Their area, at the same time, remains constant. Thus, the invariant for a long bar must correspond to the invariant for a short bar.

Let us define the invariant for a long bar and take as a basis the linear cohesive law [6] like the following

$$\tau(x) = a \cdot \sigma(x) + b. \qquad (2)$$

From the equation of compatibility of deformations, we obtain

$$\frac{ds}{dx} = \varepsilon_s = \frac{\sigma}{E_s} \quad \Rightarrow \quad ds = \frac{\sigma}{E_s} dx. \qquad (3)$$

From the equation of equilibrium of the bar

$$\frac{d\sigma}{dx} = \frac{u_p}{A_s} \cdot \tau(x). \qquad (4)$$

To simplify the equation, we introduce the expression

$$k = \frac{u_p}{A_s} = \frac{4}{d}. \qquad (5)$$

We rewrite the equation (4), taking into account (2) and (5) as follows

$$dx = \frac{d\sigma}{k(a \cdot \sigma + b)}. \qquad (6)$$

We enterequation (6) into formula (3)

$$ds = \frac{\sigma d\sigma}{k \cdot E_s \cdot (a \cdot \sigma + b)}. \qquad (7)$$

We define the cohesion invariant

$$G_{tot} = \int \tau(s) ds = \frac{1}{k \cdot E_s} \int_0^{f_y} \frac{(a \cdot \sigma + b)\sigma}{a \cdot \sigma + b} d\sigma = \frac{f_y^2}{2 \cdot k \cdot E_s}. \qquad (8)$$

The physical meaning of the obtained value of the invariant indicates that the invariant determines the area of the τ-s diagram, and therefore does not depend on the shape of the diagram and, accordingly, on the coefficients a and b. It can be finally concluded that the performance of the cohesive forces is equal to the potential energy of deformation of the stretched bar. In addition, the value of the invariant does not depend on the cohesive law, but is determined by the energy consumption of the reinforcement bar. It becomes obvious that the invariant does not depend on the form of the stress diagram. It means that the cohesion forces appliedin the force transmission area are equivalent to the potential energy of deformation of the reinforcement bar.

The elementary work of the cohesion forces dA on the displacement ds is determined by the equation

$$dA = \tau(s) \cdot u \cdot dx \cdot ds, \qquad (9)$$

where u is the perimeter of the bar.

The specific work per area unit of the cross-section part of the reinforcement As is equal to

$$dG = \frac{dA}{A_s} = \tau(s) \cdot k \cdot ds \cdot dx. \qquad (10)$$

Taking into account the equation of compatibility of deformations (3) and the equation of equilibrium of the bar (4), the potential energy of deformation of the bar will be equal to

$$G(\sigma) = \int_0^{\sigma} \tau(\sigma) \cdot \frac{\sigma}{E_s} \cdot \frac{d\sigma}{k \cdot \tau(\sigma)}. \qquad (11)$$

After simple transformations, we obtain the value of the fundamental cohesive invariant

$$G(\sigma) = \frac{1}{k \cdot E_s} \int_0^{\sigma} \sigma d\sigma = \frac{\sigma^2}{2 \cdot k \cdot E_s}. \qquad (12)$$

This confirms the validity of the formulated hypotheses.

For short rods, two deformation plots must be implemented. In the first plot, the applied linear

cohesive law (2) must operate, and in the second plot, the cohesive stresses must be assumed to be constant.

Let us define the invariant value in the second plot under constant cohesion values with the help of the equilibrium equation

$$\frac{d\sigma}{dx} = k \cdot \tau_{\max}. \quad (13)$$

After simple transformations,

$$dx = \frac{d\sigma}{k \cdot \tau_{max}}. \quad (14)$$

We enter the equation for dx from equation (10) into equation (3)

$$ds = \frac{\sigma}{E_s} \cdot \left(\frac{d\sigma}{k \cdot \tau_{max}} \right) = \frac{1}{E_s \cdot k \cdot \tau_{max}} \cdot \sigma \cdot d\sigma. \quad (15)$$

We calculate the cohesive invariant in the second plot at constant coupling values

$$G_2 = \int \tau(s) ds = \frac{1}{k \cdot E_s} \frac{\tau_{\max}}{\tau_{\max}} \int_{\sigma_1}^{f_y} \sigma d\sigma = \frac{f_y^2 - \sigma_1^2}{2 \cdot k \cdot E_s}. \quad (16)$$

Thus, wedevelop the energy balance formula for a short bar

$$G_{tot} = G_1 + G_2 = \frac{\sigma_1^2}{2 \cdot k \cdot E_s} + \frac{f_y^2 - \sigma_1^2}{2 \cdot k \cdot E_s} = \frac{f_y^2}{2 \cdot k \cdot E_s}. \quad (17)$$

If we denote the 'energy contribution' of the second plot as the conditional square of the stress $\sigma_2^2 = f_y^2 + \sigma_1^2$, we finally obtain

$$\sigma_1^2 + \sigma_2^2 = f_y^2. \quad (18)$$

Thus, a conditionally short bar has two plots

– plot 1 from 0 to L_1, where the linear law works (2);

– plot 2 from L_1 до L, where tangential stresses are constant and mean $\tau = \tau_u$=const.

Normal stresses in the reinforcement in:

1. plot 1

$$\sigma_1 = \frac{b}{a}(e^{akL_1} - 1). \quad (19)$$

$$\tau(x) = b \cdot e^{a \cdot k \cdot x} = b \cdot e^{4\frac{a}{d} \cdot x}. \quad (20)$$

Equation (19) is derived by integrating equation (6).

2. plot 2

$$\sigma_2 = k \cdot \tau_u \cdot (L - L_1). \quad (21)$$

Equation (21) is derived from equation (13).

At the transition point at lengthL_1, the cohesive stresses reach a maximum, i.e.

$$\tau_u = a\sigma_1 + b. \quad (22)$$

In this case, the total stress must be equal to the yielding point

$$\sigma_{total} = \sigma_1 + \sigma_2 = f_y. \quad (23)$$

To determine the maximum tangential stress τ_{max}, it is necessary to determine the value of L_1. To do this, let us first establish the stress σ_1 from equation (22) and enter it into equation (19). After simple transformations, we obtain

$$L_1 = \frac{1}{a \cdot k} \ln\left(\frac{\tau_u}{b} \right). \quad (24)$$

Finally, equation (23) takes the following form

$$\frac{\tau_u - b}{a} + k \cdot \tau_u \cdot \left(L - \frac{1}{a \cdot k} \ln \frac{\tau_u}{b} \right) = f_y. \quad (25)$$

Solving equation (25), we obtain the value of τ_u. It is worth noting that the solution of equation (25) indicates the absence of a horizontal section. This points out the inconsistency of the set law in the form of (2) over the entire span of the bar's operation.

The given law is valid only for certain stresses σ_1. Therefore, the definition of the parameter a through the yielding point is incorrect. When the stresses σ_1 are reached, the tangential stresses will reach $\tau_1=\gamma\tau_u$. To determine the parameter γ, we will accept a theoretical hypothesis that the plastic stage begins when the increase in cohesive stresses τ_1-b becomes equal to the residual strength τ_u-τ_1. It means that τ_1 corresponds to the point of maximum energy efficiency of the elastic diagram. To confirm this hypothesis, we will apply the principle of equality of intensities of energy invariants of the elastic and plastic stages of adhesion. Since most software packages include tabular values of the τ-s dependence, which correspond to segmented linear diagrams, we will therefore propose a method based on a two-line diagram. Let us assume that in the first plot, the dependence τhas the following form

$$\tau = j \cdot s + b. \quad (26)$$

In this case, the invariant will include two items

$$G_{tot} = \int_0^{s_u} \tau(s) ds = G_1 + G_2, \quad (27)$$

where G_1 is the energy accumulated in the elastic plot, and G_2 is the energy spent in the plastic plot.

Let us define the cohesive invariant in the first plot (the area of the trapezium below the graph τ-s)

$$G_1 = \int_0^{s_1} (j \cdot s + b) ds = \frac{j \cdot s_1^2}{2} + b \cdot s_1. \quad (28)$$

Let us define the cohesive invariant in the second plot (the area of the rectanglebelow the graph τ-s)

$$G_2 = \int_{s_1}^{s_u} \tau(s) ds = \tau_u (s_u - s_1). \quad (29)$$

The criterion of energy optimality means the ability of the system to make maximum use of the elastic stage without losing the overall load-bearing capacity, as follows

$$\frac{d}{ds_1}\left(\frac{G_1}{G} \right) = 0. \quad (30)$$

According to the rules of differentiation, we obtain

$$\frac{dG_1}{ds_1} \cdot G - G_1 \cdot \frac{dG}{ds_1} = \\ = \frac{dG_1}{ds_1} \cdot (G_1 + G_2) - G_1 \cdot \left(\frac{dG_1}{ds_1} + \frac{dG_2}{ds_1} \right) = 0. \quad (31)$$

After simple transformations,

$$\frac{1}{G_1} \frac{dG_1}{ds_1} = \frac{1}{G_2} \frac{dG_2}{ds_1}. \quad (32)$$

Let us define the derivatives of the corresponding invariants

$$\frac{dG_1}{ds_1} = j \cdot s_1 + b = \tau_1; \quad (33)$$

$$\frac{dG_2}{ds_2} = -\tau_u. \quad (34)$$

In this case,

$$\frac{\tau_1}{G_1} = \frac{\tau_u}{G_2}. \quad (35)$$

Let us define the limit slip s_u in terms of maximum cohesion. Since $\tau_u = j\, s_u + b$, then

$$s_u = \frac{\tau_u - b}{j}. \quad (36)$$

Finally, equation (34) takes the following form

$$\frac{j \cdot s_1 + b}{\frac{j \cdot s_1^2}{2} + b \cdot s_1} = \frac{1}{s_u - s_1}. \quad (37)$$

After simple algebraic transformations (37) andaccounting (36), we obtain the validation of the suggested hypothesis

$$\tau_1 - b = \tau_u - \tau_1 \Rightarrow \tau_1 = \frac{\tau_u + b}{2}. \quad (38)$$

Equation (38) allows us to get the coefficient of the value γ

$$\gamma = \frac{\tau_u + b}{2\tau_u} = 0.5 + \frac{b}{2\tau_u}. \quad (39)$$

Let us define another coefficient j that determines the ratio of the increase in cohesive stresses to the increase in slip at a given point

$$j = \frac{d\tau}{ds}. \quad (40)$$

Let us find the derivative of the function τ(x) along the length of the bar

$$\frac{d\tau}{dx} = a\frac{d\sigma}{dx} = a(k\tau) = a \cdot k \cdot \tau. \quad (41)$$

The derivative of the function τ(x) we represent by the slip

$$\frac{d\tau}{dx} = \frac{d\tau}{ds} \cdot \frac{ds}{dx} = j \cdot \varepsilon_s = j \cdot \frac{\sigma}{E}. \quad (42)$$

After realting equations (40) and (41) we obtain

$$a \cdot k \cdot \tau = \frac{j \cdot \sigma}{E} \Rightarrow j = \frac{a \cdot k \cdot \tau \cdot E}{\sigma}. \quad (43)$$

Let us substitute the value of σ from the basic law into equation (2)

$$a \cdot k \cdot \tau = \frac{j \cdot \sigma}{E} \Rightarrow j = \frac{a \cdot k \cdot \tau \cdot E}{\sigma}. \quad (44)$$

Then, let us use the energy invariant for the transition point and insert expression τ_1 (38) into equation (44)

$$j = a^2 \cdot E \cdot k \cdot \frac{\frac{\tau_u + b}{2}}{\frac{\tau_u + b}{2} - b} = a^2 \cdot E \cdot k \cdot \frac{\tau_u + b}{\tau_u - b}. \quad (45)$$

Let us establish the limit values of the parameters of the cohesion of reinforcement to concrete:

– the limit values of the cohesion stresses are

$$\tau_u = \eta_1 \eta_2 f_{ctm}. \quad (46)$$

– the limit length of the barat which it is able to perceive stresses equal to the yielding stress

$$L_u = \frac{f_y}{k \cdot \tau_u}. \quad (47)$$

Coefficient b, which characterises the parameters of the initial cohesive strength and physically describes the cohesion force, also describes initial mechanical cohesion, isdefined by the equation

$$b = \alpha_0 f_{ctm} = 0.4 \cdot f_{ctm}. \quad (48)$$

Coefficient b integrates three main physical phenomena that occur at the steel-concrete contact before the onset of active slippage:

– chemical cohesion means bonding of cement stone to the reinforcement surface at the molecular level.

– friction forces from shrinkage as concrete contracts during hardening, squeezing the bar and creating initial friction.

– initial mechanical resistance of the surface irregularities of the reinforcement.

Coefficient a,which characterizes the intensity of stresses transfer, is defined from the condition of the appearance of stresses $\sigma_1$at the loaded end when the stresses are distributed over the length L_u. For doing this, we will use equation (20) to define a

$$\tau_1 = b \cdot e^{akL_u} \Rightarrow a = \frac{1}{k \cdot L_u} \ln\left(\frac{\gamma \cdot \tau_u}{b}\right). \quad (49)$$

The final equation for finding coefficient a is obtained by substituting the kL_u values from equation (46) into formula (47)

$$a = \frac{\tau_u}{f_y} \ln\left(\frac{\gamma \cdot \tau_u}{b}\right). \quad (50)$$

The division into short and long bars occurs by the comparison of the anchoring length with the limit length L_u.

The bars are considered conditionally short under the general anchoring length L less than L_u ($L<L_u$). In the short bars, the stresses reach the free end of the reinforcement quickly. In the reinforcement, the stresses do not reach the yielding strength f_y, so failure occurs due to the reinforcement pulling out of the concrete.

The first stage of the short bars'performance (Elastic). The cohesion stresses are distributed according to the exponential law. As the bar is short, the stresses on the free end (x=0) quickly become more than zero. At this stage, the tangential stress is determined by equation (26). The displacement corresponding to the tangential stress $\tau_1$is determined by the expression

$$s_1 = \frac{b}{j}\left(e^{a \cdot k \cdot L} - 1\right). \quad (51)$$

The second stage of the short bars'performance (Elasto-plastic). This stage starts from the moment when the stresses on the loaded end reach τ_1, and the active length corresponds to the physical one, $L_{act} = L$. The stress diagram is already unable to expand further, so it begins to change its form. Destruction occurs when $\tau_p = \tau_u$ across the entire contact area. The stresses in the reinforcement do not reach the yielding point $\sigma<f_y$. When the stresses front reaches the free end of the anchor (x=L), the free end loses its immobility. This leads to a transformation of the global stiffness parameters of the system, from the pure cohesive stiffness j to the reduced stiffnessJ_f, which takes into account the simultaneous shear and tension of the bar along the entire anchoring length. The global stiffness j is defined as the tangent of the slope of the τ-s diagram in the second plot. Mathematically, it is the derivative of the tangential stresses over the slip

$$J_f = \frac{d\tau_{load}}{ds}. \quad (52)$$

When the whole bar is working, global slip at the loaded end s corresponds to the slip caused by the average stresses level τ_{avg} along the length L

$$s = \frac{\tau_{avg}}{j}. \quad (53)$$

The cohesive stresses distribution along the bar τ obeys the exponential law, which follows from the differential equation of equilibrium. The cohesive stresses along the length of the bar are determined by the equation

$$\tau(x) = b_{ef} \cdot e^{akx}. \quad (54)$$

where b_{ef} meanstangential stressesin the second plot at the free end.

The stresses at the loaded end x=L

$$\tau_{load} = b_{ef} \cdot e^{akL} \Rightarrow b_{ef} = \tau_{load} \cdot e^{-akL}. \quad (55)$$

Thus, the distribution along the bar

$$\tau(x) = \tau_{load} \cdot e^{-ak(L-x)}. \quad (56)$$

Now, let us define the average stresses

$$\tau_{avg} = \frac{1}{L}\int_0^L \tau(x)dx = \frac{1}{L}\int_0^L \tau_{load} \cdot e^{-ak(L-x)}dx. \quad (57)$$

Let us calculate the integral of equation (57)

$$\int_0^L e^{akx}dx = \left[\frac{e^{akx}}{ak}\right]_0^L = \frac{e^{akL}-1}{ak}. \quad (58)$$

Finally, the average stresses are calculated by the equation

$$\tau_{avg} = \tau_{load} \cdot \frac{1-e^{-akL}}{akL}. \quad (59)$$

We enterthe received result (59) in the equation (53)

$$s = \frac{\tau_{load} \cdot (1-e^{-akL})}{j \cdot akL} \Rightarrow \tau_{load} = s \cdot \frac{j \cdot akL}{1-e^{-akL}}. \quad (60)$$

Finally, the reduced stiffness in the second plot is calculated by the equation

$$J_f = j \cdot \frac{akL}{1-e^{-akL}}. \quad (61)$$

The displacement in the second plot is calculated by the expression

$$s_2 = s_1 + \frac{\tau_u - \tau_1}{J_f}. \quad (62)$$

The long bars correspondto the condition $L \geq L_u$. They have a considerable length, which means thatthe stresses in the reinforcement reach the yielding point f_y earlier than the free end of the reinforcement begins to displace.

The first stage of the long bars'performance (Elastic). The active length L_{act} of stress distribution increases gradually, but it is less than the physical length of the bar L. The free end remains unstressed. At this stage, the slip function is also piecewise linear, but the 'break' point is determined by the strength of the contact layer $\tau_1=\gamma\tau_u$. The tangential stresses are also determined by equation (26).

The second stage of the long bars' performance (Plastic). Plastic deformations emerge when the loaded end reaches stresses τ_1. The length of the plastic zone L_2 is growing, while the elastic one remains constant (equal to L_u). The bar is not pulled out. Instead, the reinforcement stresses reach the yielding limit f_y. This safe plastic failure is a priority in design. Plastic deformations appear in this area.

Slippage at the loaded end s consists of slippage at the boundary of the two zones and additional elongation of the reinforcement in the plasticity plot, so the following can be written

$$s = s_1 + \Delta s_{pl}. \quad (63)$$

In the plastic plot, the cohesive stresses are constant, due to what the stresses in the reinforcement are changing lineary

$$\sigma(x) = \sigma_1 + \frac{du \cdot \tau_p}{A_s} \cdot x = \sigma_1 + k \cdot \tau_p \cdot x, \quad (64)$$

where x is the distance from the boundary of zone L_1, and $\sigma_1 = (\tau_p - b)/a$.

We integrate the deformations $\varepsilon(x) = \sigma(x)/E$ along the length of the bar

$$\Delta s_{pl} = \int_0^{L_2} \frac{\sigma_1 + k\tau_p x}{E}dx = \left[\frac{\sigma_1 x}{E} + \frac{k\tau_p x^2}{2E}\right]_0^{L_2}. \quad (65)$$

and finally get

$$\Delta s_{pl} = \int_0^{L_2} \frac{\sigma_1 + k\tau_p x}{E}dx = \left[\frac{\sigma_1 x}{E} + \frac{k\tau_p x^2}{2E}\right]_0^{L_2}. \quad (66)$$

The tangential stresses τ_p are calculated from the condition that the yielding point f_y is reached in the reinforcement. The stresses in the reinforcement σ is calculated by the area of the stress diagram ω

$$\sigma = k \cdot \omega = k \cdot (\omega_{el} + \omega_{pl}). \quad (67)$$

The relevant areas of elastic and plastic plots equal

$$\omega_{el} = \int_0^{L_1} b \cdot e^{akx}dx = \frac{\tau_p - b}{ak}; \quad (68)$$

$$\omega_{pl} = \tau_p \cdot L_2. \quad (69)$$

Thus, the general equation for calculating the stresses in the reinforcement will take the following form

$$\sigma = k \cdot \left[\frac{\tau_p - b}{ak} + \tau_p \cdot (L - L_1) \right]. \quad (70)$$

To calculate tangential stresses τ_p,we need to set the limit conditions for the equation (70) $\sigma=f_y$, $L_1=L_u$. In this case, we obtain the equation for calculating tangential stresses τ_p.

$$\tau_p = \frac{a \cdot f_y + b}{1 + a \cdot k \cdot (L - L_u)}. \quad (71)$$

It is worth noting that the plastic performance of concrete may not occur for extremely long bars. The latter equation (71) allows to set the limit point of the length $L_{cr,}$ after which a plastic plot will be absent at all. We can calculate it by using $\tau_p=\tau_1$ in equation (71) and thus receive the appropriate bar length

$$L_{cr} = L_u + \frac{\tau_u \cdot \ln\left(\frac{\gamma\tau_u}{b}\right) + b - \gamma\tau_u}{a \cdot k \cdot \gamma\tau_u}. \quad (72)$$

The length L_{cr} divides all long bars ($L > L_u$) into two groups according to their failure character:

1. $L_u < L < L_{cr}$:The stresses in the reinforcement will reach the yielding point (f_y) when the concrete enters the plastic stage ($\tau_p>\tau_1$). This is the most common case for standard anchoring. The stress diagram will have a clearly defined plasticity plot L_2.
2. $L > L_{cr}$. The bar is so long that the stresses in the reinforcement will have reached the yielding point (f_y) before the plastic deformations will develop in the concrete. This means that the concrete around such an anchor is always in its elastic stage, and the bond diagram at the moment f_y has the form of an exponential.
3. $L = L_{cr}$. This is the state of "a perfect balance", where the achievement of the yielding point (f_y) in the reinforcement exactly corresponds to the energy threshold for the onset of plastic deformation of the concrete (τ_1).

Let us show an example of constructing the "τ - s" displacement diagrams for three samples with the following parameters:

– the concrete type C25/30, f_{ctm} = 1.99 MPa (average tensile strength).

– the reinforce type A500, f_{yd} = 435 МПа, $E_s = 2\times10^5$MPa.

1. The first sample with diameter d = 10 mm, L=100 mm.
2. The second sample with diameter d = 10 mm, L=200 mm.
3. The third sample with diameter d = 10 mm, L=300 mm.

The parameters of the diagram for the first sample:

1. The parameters of the linear model a=0.0147, b=0.80 MPa;
2. The parameters of the diagram s_1=0.026 mm, τ_1=1.435 MPa;
3. The parameters of the diagram s_2=0.188 mm, τ_2=4.482 MPa;

The parameters of the diagram for the second sample:

1. The parameters of the linear model a=0.0147, b=0.80 MPa;
2. The parameters of the diagram s_1=0.072 mm, τ_1=2.585 MPa;
3. The parameters of the diagram s_2=0.202 mm, τ_2=4.482 MPa;

The parameters of the diagram for the third sample:

1. The parameters of the linear model a=0.0147, b=0.80 MPa;
2. The parameters of the diagram s_1=0.074 mm, τ_1=2.640 MPa;
3. The parameters of the diagram s_2=0.214 mm, τ_2=3.934 MPa.

General view of the diagrams «τ - s» are given in Fig 1.

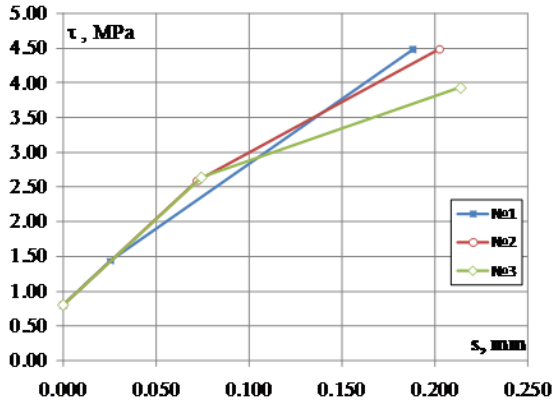

Figure 3 – Diagrams of the dependence of "τ - s" of average tangential shear stresses on shear strains

Interpretation of results and their approval.

The obtained diagrams are used for modelling the cohesion in computational software packages developed on the basis of the finite element method. In further studies, we will show their use in modelling the operation of reinforced concrete elements and calculating loop joints. Also, if necessary, it is possible to develop a method for constructing a horizontal section of the "τ - s" diagram for which the stresses increase from the yielding point f_y to the strength limit of the reinforcement f_u.

Conclusions.

The main scientific novelty of the article is the substantiation of the following phenomenon: the transition point from the stage of elastic work to the stage of plastic work is not a random value, but a point of energy optimization. The system receives plastic deformations when the increase in elastic energy becomes equal to the intensity of the plastic resource ($2\tau_1 = \tau_u + b$). A single mathematical apparatus has been developed for bars of different lengths. Until now, the scientists often separated the methods for short anchors and long cohesiveplots. The suggested method

made it possible to describe the cross-cuttingslipping function τ-s, which:

– for short bars ($L < L_u$), describes the mechanics of the reinforcement pulling out due to the changes in the form of the force diagram.

– for long bars ($L \geq L_u$), describes the performance of the reinforcement from its starting point to its tangential point (f_y), taking development of plastic deformations into account.

The study specifies the parameters of cohesive stiffness. The derived formula for calculating j takes into account the quality of contact at the micro level, which will significantly increase the accuracy of deformation calculations compared to other simplified models. The suggested methodology will allow to accurately calculate the minimum required anchoring length (L_u), which guarantees that the reinforcement reaches the yielding point, including for loop joints; to simulate real slippage of reinforcement in cracks in reinforced concrete constructions, which is important for calculating the width of crack opening and deflections; to determine the 'energy reserve' of the cohesion for constructions operating in difficult conditions (for example, under dynamic loads).

References

1. Al-Mahmoud, A., & Mazher, A. (2024). Experimental study of bond-slip relationships in high-performance self-consolidating concrete with plain steel bars. Engineering Structures, 319, Article 118854. https://doi.org/10.1016/j.engstruct.2024.118854
2. Щодо оцінювання зчеплення арматури з бетоном / О. В. Ромашко, В. Н. Ромашко // Збірник наукових праць Українського державного університету залізничного транспорту. - 2018. - Вип. 179. - С. 92-99. https://doi.org/10.18664/1994-7852.179.2018.147756
3. Ariyaratnam, S. N., & Pande, G. N. (2015). Bond slip model in cylindrical reinforced concrete elements confined with stirrups. International Journal of Advanced Structural Engineering, 7, 365–375. https://doi.org/10.1007/s40091-015-0104-7
4. Hsiao, P.-C., Chen, I.-S., & Hwang, P.-A. (2025). Assessment of the experimental and numerical bond–slip law of various strengthening systems in reinforced concrete elements. International Journal of Concrete Structures and Materials, 19, Article 92. https://doi.org/10.1186/s40069-025-00838-5
5. Karadogan, Z., Elchalakani, M., & Mirza, S. M. (2022). Validation of reinforced concrete bond stress–slip models through an analytical strain distribution comparison. Materials and Structures, 55, Article 240. https://doi.org/10.1617/s11527-022-02071-y
6. Kochkarov D.V. Neliniinyi opir zalizobetonnykh elementiv i konstruktsii sylovym vplyvam: Monohrafiia. – Rivne: O. Zen, 2015. – 384 s.:Il.: 139; tabl. 48; bibliohr: 326 - ISBN 978-617-601-125-5.
7. R. Eligehausen, E. P. Popov, and V. V. Bertero, "Local Bond Stress–Slip Relationships of Deformed Bars under Generalized Excitations," Report No. UCB/EERC-83/23, Earthquake Engineering Research Center, University of California, Berkeley, 1983.
8. Comité Euro-International du Béton (CEB), CEB-FIP Model Code 1990: Design Code, Thomas Telford, London, 1993.
9. FIB (Fédération internationale du béton), FIB Model Code for Concrete Structures 2010, Ernst & Sohn, Berlin, 2013.
10. EN 1992-1-1, Eurocode 2: Design of Concrete Structures – Part 1-1: General Rules and Rules for Buildings, CEN, Brussels, 2004.
11. Tang, C. W., & Cheng, C. K. (2020). Modeling Local Bond Stress-Slip Relationships of Reinforcing Bars Embedded in Concrete with Different Strengths. *Materials (Basel, Switzerland)*, *13*(17), 3701. https://doi.org/10.3390/ma13173701

1. Al-Mahmoud, A., & Mazher, A. (2024). Experimental study of bond-slip relationships in high-performance self-consolidating concrete with plain steel bars. Engineering Structures, 319, Article 118854. https://doi.org/10.1016/j.engstruct.2024.118854

2. Romashko, O. V., & Romashko, V. N. (2018). On the assessment of reinforcement–concrete bond. Collection of Scientific Works of the Ukrainian State University of Railway Transport, 179, 92–99. https://doi.org/10.18664/1994-7852.179.2018.147756

3. Ariyaratnam, S. N., & Pande, G. N. (2015). Bond slip model in cylindrical reinforced concrete elements confined with stirrups. International Journal of Advanced Structural Engineering, 7, 365–375. https://doi.org/10.1007/s40091-015-0104-7
4. Hsiao, P.-C., Chen, I.-S., & Hwang, P.-A. (2025). Assessment of the experimental and numerical bond–slip law of various strengthening systems in reinforced concrete elements. International Journal of Concrete Structures and Materials, 19, Article 92. https://doi.org/10.1186/s40069-025-00838-5
5. Karadogan, Z., Elchalakani, M., & Mirza, S. M. (2022). Validation of reinforced concrete bond stress–slip models through an analytical strain distribution comparison. Materials and Structures, 55, Article 240. https://doi.org/10.1617/s11527-022-02071-y
6. Kochkarov D.V. Neliniinyi opir zalizobetonnykh elementiv i konstruktsii sylovym vplyvam: Monohrafiia. – Rivne: O. Zen, 2015. – 384 s.:Il.: 139; tabl. 48; bibliohr: 326 - ISBN 978-617-601-125-5.
7. R. Eligehausen, E. P. Popov, and V. V. Bertero, "Local Bond Stress–Slip Relationships of Deformed Bars under Generalized Excitations," Report No. UCB/EERC-83/23, Earthquake Engineering Research Center, University of California, Berkeley, 1983.
8. Comité Euro-International du Béton (CEB), CEB-FIP Model Code 1990: Design Code, Thomas Telford, London, 1993.
9. FIB (Fédération internationale du béton), FIB Model Code for Concrete Structures 2010, Ernst & Sohn, Berlin, 2013.
10. EN 1992-1-1, Eurocode 2: Design of Concrete Structures – Part 1-1: General Rules and Rules for Buildings, CEN, Brussels, 2004.
11. Tang, C. W., & Cheng, C. K. (2020). Modeling Local Bond Stress-Slip Relationships of Reinforcing Bars Embedded in Concrete with Different Strengths. *Materials (Basel, Switzerland)*, *13*(17), 3701. https://doi.org/10.3390/ma13173701

12. K. Lundgren, Bond between ribbed bars and concrete. Part 2: The effect of corrosion,"*Magazine of Concrete Research*, vol. 57, no. 7, pp. 383–395, 2005. https://doi.org/10.1680/macr.2005.57.7.383
13. Kang S, Tan KH (2016), Bond–slip behaviour of deformed reinforcing bars embedded in well-confined concrete. *Magazine of Concrete Research*, Vol. 68 No. 10 pp. 515–529. https://doi.org/10.1680/jmacr.15.00245
14. Mang C, Jason L, Davenne L (2015), A new bond slip model for reinforced concrete structures: Validation by modelling a reinforced concrete tie". *Engineering Computations*, Vol. 32 No. 7 pp. 1934–1958, doi: https://doi.org/10.1108/EC-11-2014-0234
15. Wang, Y., & Qiao, J. (2024). Research progress of bond slip at the interface of FRP bars and concrete. *Academic Journal of Science and Technology*, 9(3), 25–29. https://doi.org/10.54097/7s3rba19
16. Xiao, J., & Wu, H. (2021). Experimental study on the bond-slip behavior and stress transfer mechanism between shaped steel and high-performance fiber-reinforced concrete. *Structures*, 34, 5013–5028. https://doi.org/10.1016/j.istruc.2021.09.014

12. K. Lundgren, "Bond between ribbed bars and concrete. Part 2: The effect of corrosion," *Magazine of Concrete Research*, vol. 57, no. 7, pp. 383–395, 2005. https://doi.org/10.1680/macr.2005.57.7.383
13. Kang S, Tan KH (2016), Bond–slip behaviour of deformed reinforcing bars embedded in well-confined concrete. *Magazine of Concrete Research*, Vol. 68 No. 10 pp. 515–529. https://doi.org/10.1680/jmacr.15.00245
14. Mang C, Jason L, Davenne L (2015), "A new bond slip model for reinforced concrete structures: Validation by modelling a reinforced concrete tie". *Engineering Computations*, Vol. 32 No. 7 pp. 1934–1958, doi: https://doi.org/10.1108/EC-11-2014-0234
15. Wang, Y., & Qiao, J. (2024). Research progress of bond slip at the interface of FRP bars and concrete. *Academic Journal of Science and Technology*, 9(3), 25–29. https://doi.org/10.54097/7s3rba19
16. Xiao, J., & Wu, H. (2021). Experimental study on the bond-slip behavior and stress transfer mechanism between shaped steel and high-performance fiber-reinforced concrete. *Structures*, 34, 5013–5028. https://doi.org/10.1016/j.istruc.2021.09.014

Suggested Citation:

APA style: Hryshchenko, O., & Kochkarev, D. (2025). Invariance of reinforcement and concrete cohesion within the energy approach. *Academic Journal Industrial Machine Building Civil Engineering*, *2*(65), 68–76. https://doi.org/10.26906/znp.2025.65.4212

DSTU style: Hryshchenko O., Kochkarev D. Invariance of reinforcement and concrete cohesion within the energy approach. *Academic journal. Industrial Machine Building, Civil Engineering*. 2025. Vol. 65, iss. 2. P. 68–76. URL: https://doi.org/10.26906/znp.2025.65.4212.

Грищенко О.Д.
Національний університет водного господарства та природокористування
https://orcid.org/0009-0004-1851-6571

Кочкарьов Д.В.*
Національний університет водного господарства та природокористування
https://orcid.org/0000-0002-4525-7315

Інваріантність зчеплення арматури з бетоном на основі енергетичного підходу

Аннотація. У роботі розглянуто проблему аналітичного опису зчеплення арматури з бетоном при висмикуванні, яка є визначальною при оцінюванні піддатливості петлевих стиків і стикових з'єднань збірних залізобетонних конструкцій. Показано, що в таких з'єднаннях передача зусиль між елементами відбувається переважно за рахунок роботи зчеплення, що зумовлює високу чутливість розрахункових параметрів до прийнятого закону взаємодії «арматура–бетон». Аналіз існуючих експериментальних, напівемпіричних і нормативних моделей зчеплення свідчить про їх обмежену здатність описувати вплив нормальних напружень в арматурі та стадію насичення зчеплення, яка супроводжується зміною форми епюри дотичних напружень уздовж довжини анкерування. У статті запропоновано універсальну аналітичну модель зчеплення, яка базується на поєднанні локальної лінійної залежності між дотичними та нормальними напруженнями на початковій стадії роботи і горизонтальної пластичної ділянки, що відповідає пластичній стадії роботи (розвиненого механічного зачеплення). Ключовим елементом моделі є введення енергетичного інваріанта зчеплення, який ототожнюється з питомою енергією пружної деформації арматури та не залежить від довжини анкерування. Для визначення точки переходу від пружної до пластичної стадії сформульовано принцип еквівалентності інтенсивностей енергетичних інваріантів, який дозволяє інтерпретувати початок пластичної течії як стан максимальної енергетичної ефективності пружної епюри. На цій основі отримано аналітичну умову, що пов'язує граничні дотичні напруження зчеплення з рівнем адгезії та залишковим ресурсом міцності. Запропонований підхід забезпечує побудову фізично обґрунтованих діаграм типу «дотичні напруження – зміщення», придатних для використання в чисельних методах розрахунку піддатливості стиків і дозволяє усунути заниження несучої здатності коротких анкерів, характерне для традиційних моделей. В роботі показано приклади побудови діаграм «дотичні напруження – зміщення» для трьох зразків із різною довжиною арматурних стержнів.

Ключові слова: діаграми зсуву, моделі зчеплення арматури з бетоном, деформації зсуву, параметри зчеплення, середні дотичні напруження зчеплення.

*Адреса для листування E-mail: dim7@ukr.net

Надіслано до редакції:	04.11.2025	Прийнято до друку після рецензування:	05.12.2025	Опубліковано (оприлюднено):	26.12.2025